TSICNet: Importance of Connectome Information for Epilepsy Classification

Zonghan Du[1] and Zhongyuan Lai[2]

[1] School of Computer Science, Sun Yat-sen University, Guangzhou 510275, China
duzh9@mail2.sysu.edu.cn
[2] DeepVerse Inc., Shanghai 200135, China
abrikosoff@yahoo.com

Abstract. Epilepsy is a chronic brain disease characterized by recurrent seizures. These episodes are usually triggered by abnormal firing of neurons in the brain and appear as brief, recurring episodes. From the point of view of mitigation and treatment, a major problem is timely and accurate classification of epileptic seizure episodes, which is important for rapid intervention and possible prevention of future episodes. In recent years, with the rapid development of artificial intelligence technology, its application in the field of epilepsy diagnosis is increasingly extensive. In particular, electroencephalography (EEG), as a non-invasive neurophysiological examination method, plays an important role in the diagnosis of epilepsy. In particular, it allows the learning of *connectomic* information from the relative positions of EEG electrodes on the scalp. In this paper, a deep learning model, **T**emporal-**S**patio-**I**mportance **C**orrelation **N**etwork (TSICNet), is proposed to classify the onset of epileptic seizures. Our model design combines a variety of neural network components and training methods, such as graph, spatio-temporal and separable convolutional networks, as well as sliding windows data extraction techniques and ATCNet's time-sensitive attention mechanism, to realize effective recognition and extraction of epilepsy data features. In particular, TSICNet makes heavy use of learned connectomic information to enhance classification accuracy. Experimental results show excellent performance on the CHB-MIT Scalp EEG dataset and HUH neonatal epilpsy dataset, and has good results in accuracy and True (TPR) and False Positive Rates (FPR). Moreover, ablation analysis shows that each part of the model contributes significantly, thus confirming the validity our design principles.

Keywords: Electroencephalogram · Connectome · Epilepsy Classification · Graph Neural Networks

1 Introduction

Epilepsy is one of the most common neurological diseases [32]. The most recognizable symptom of epilepsy are frequent and often severe *seizures*. The effects of an episode can range from minor lapses in attention [27] to abnormal movements

(convulsions) of patients' body, in the sense that they lost partial or complete control. Such episodes could also entail loss of consciousness, bowel control, cognitive functions and sensations [4]. Patients' actions while within these abnormal periods will potentially endanger their physical well-being, and a particularly severe episode could lead to injury or even death. In the twentieth century, epilepsy has become one of the most prevalent neurological ailments; its sociological and economic costs are substantial, since it affects 50 million people globally, and out of the three million afflicted in the United States, around $450,000$ are under the age of 17. In this sense, epilepsy incurs a substantial social cost as well [7]. In addition, there is also social stigma associated to people suffering from epilepsy, in the sense that they are often perceived to be "uncontrollable" or uninhibited [4], a phenomena which is directly related to the strong link between epilepsy and the frequency of seizures. If untreated, it is also often fatal: patients are usually unaware of their predicament until too late. However, if discovered early, epileptic fits can be addressed sufficiently via medications [19]; however, the efficacy of such interventions depends critically on early diagnosis of epilepsy. Conventional diagnostic techniques are mainly based on after-the-event curative techniques, which focusses on medical intervention *after* an epileptic episode. However, such measures have been widely acknowledged to be inadequate for cases where the first episode might be the most severe, and which severity will gravely influence the frequency and intensity of all subsequent epileptic episodes. Hence, the *diagnosis* of epileptic seizures has become a crucial but still unsolved problem in the treatment of epileptic seizures.

From a neurobiological point of view, epilepsy (and, by association, epileptic seizures), can be traced to well-defined neurological sources [12]. It is known that seizures are strongly associated with abnormally excessive electrical discharges in well-defined regions of the brain [23], and, hence, can be essentially divided into three distinct types: generalized, focal and epileptic spasms [32], [27]. The first type originate in networks spanning part of one brain hemisphere, while generalized ones begin in bilateral distributed neuronal networks. These point to the overt fact that the origins of epilepsy are *strongly* spatially-dependent on brain region; in other words, the point of origin of epileptic seizures influences their later dynamics. We take this into account in the design of our model, where we enable the learning of the *connectome*, in the form of a connectivity graph extracted from the EEG signals. Having connectomic information as prior greatly increases the accuracy of our model, as we demonstrate via ablation studies.

An EEG is a trace of electrical activity of the brain, which manifests as a time series of voltage values [18]. The detection and measurement of this signal can be easily done via electrodes affixed to the scalp in a regular pattern, which has been chosen to ensure comprehensive coverage of all important regions of the brain. The voltage difference between electrodes are then measured. EEG signals have excellent temporal resolution, and hence is very suitable for diagnostic tasks, where the requirement for *timeliness* is of great importance. An EEG trace containing an epileptic episode (*ictus*) can generally be divided into four distinct states, namely *interictal*, *preictal*, *ictal* and *postictal*. Pre- and postictal are the

periods prior and subsequent to an epileptic episode, respectively, while the ictal and interictal periods refer to the interval during which an episode occurs and in-between episodes, respectively. In summary, analysis of signals collected from this set of electrodes form the clinical gold standard for diagnosis of neurological episodes.

In recent years, along with the increasing prevalence of machine and deep learning algorithms, the use these techniques to analyze EEG signals towards the aim of accurate epilepsy diagnosis has become a concrete trend. Due to the inherent complexity of the task (involving the analysis of time series data containing multiple time scales and data sources), the design of deep models which are robust and accurate, on the one hand, and interpretable, on the other, remains a challenging task. There already exist a large selection of deep models which have been optimized for the task of classifying and / or predicting epileptic seizures; some of the more recent advances in deep learning architecture (such as transformers [3]) have been deployed for this purpose as well.

Despite this wide selection of models, it is widely acknowledged that a significant barrier to the more widespread adoption of deep learning models for accurate epilepsy prediction is the lack of medical interpretability and transparent way for input of neuroscientific prior knowledge to the prediction model. In most works on the use of deep learning for epilepsy diagnosis and prediction, models are inevitably designed to be end-to-end, with no way of providing human oversight in the computational process. Apart from lack of interpretability, this black-box state of such models also make them susceptible to inaccuracies in data preprocessing and handling [16]. Such setbacks not only hamper the widespread use of deep models for fast and robust epilepsy diagnosis, it also prevents the building-up of trust in such approaches in medicine. By incorporating medical prior information in the form of a learnable connectomic graph, as well modular design of components, we aim to alleviate some of these problems in our proposed model. Our main contributions are the following:

- We present a model which is accurate and robust for epilepsy classification. We base our design principles on the importance of *connectomic* information in ensuring accuracy and performance.
- We performed extensive numerical experimentation which demonstrates the superiority of our method as compared to state-of-the-art models performing a similar task. To ensure a wide scope of data source and quality (reflecting the generalizability of our model), we evaluated our model on two different datasets covering a wide range of patient demographics;
- We show, via ablation studies, that the integration of connectomic information is crucial to achieving the SOTA performances which we display in this work. This insight can be utilized in the design of future EEG analysis frameworks, by emphasizing the importance of such information.

2 Related Work

Due to the long history and understanding of epilepsy as the most common neurological disease, there is a multitude of works relating to the traditional diagnosis and treatment, as well as more modern diagnostic approaches based on deep and machine learning, which is then directly relevant to our work. In this section we review some of these.

2.1 The Role of EEG in Epilepsy Diagnostics and Treatment

As a neurological disease, epilepsy has had a long history of diagnosis and treatment development. Medically, it is defined as a disease characterized by one or more seizures with a relatively high recurrence risk [7]. Diagnosis is based on a description of seizure behavior and EEG manifestations, further aided by neuroimaging and other genetic investigations [14]. In general, the most commonly method for diagnosis remains the recording and analysis of EEG signals [18], [30]. In this respect, clinical applications of EEG include diagnosis, selection of antiepileptic drugs (AED) therapy, evaluation of response to treatment, determination of candidacy for drug withdrawal, and surgical localization [4]. In a clinical setting, EEGs are valuable tools for epilepsy diagnosis, since they are relatively inexpensive and easy to obtain [22], [36], and contains the clearest signature of seizure onset. However, EEG signals alone are also inadequate to produce a robust and accurate diagnosis; their efficacy is affected by various clinical factors: age, seizure type, presence of AED therapy, and proximity of the EEG recording to seizure activity [12]. Hence. the accelerating shift to deep learning methods to substantially increase accuracy and robustness of diagnosis.

2.2 Deep Learning in Epilepsy Diagnosis

Since the EEG waveform consists of a time series of voltage fluctuations, it is natural to consider whether deep learning methods for time series analysis are useful for EEG analysis. In this context deep learning offers several advantages: automated detection of epileptic seizures (removing the need for manual feature engineering, which is complex for a signal as heterogeneous as a scalp EEG) [18]; the availability of large datasets with which to train such models to high levels of accuracy [14] and robustness; as well as the flexibility of designing deep learning models to take biases and priors particular to the disease into account [29], which enables clinicians to personalize models towards specific patients. In the past, a multitude of different deep models have been deployed to the task of epilepsy seizure detection. One of the earliest work by [34] used an artificial neural network for 5-class classifications of EEG segments, while [21] performs places emphasis on feature engineering by first doing clustering of the wavelet-decomposed coefficients of EEG signals before classification using a multilayer perceptron. [35] takes advantage of the expressive power of pyramidal one-dimensional convolutional neural networks for classification of the Bonn University dataset; additional architectures based on the convolutional layer are [24], [13] and [1]. There

are also models based on the analysis of time series, e.g., the models of [11] and [6] which are based on the LSTM and stacked and Bi-LSTMs, respectively.

2.3 Relevance of the Connectome to Disease Diagnostics

The connectome is an important topological input information which is increasingly receiving attention from neuroscientists as well as computer scientists. The connection between spatial information and dynamics of epileptic seizure outbreak has been studied previously and has increasingly received attention from physicians and neuoscientists [20], [23], [5]. In recent years, along with the advance in deep learning, in particular the increasing expressiveness of graph neural networks, connectomic information has also been taken into account in several early works [23], [17]. However, to our knowledge, there has not been a previous design which is able to comprehensively integrate connectomic information with pure EEG-based signals.

3 Methods

3.1 Datasets

The datasets used in this work consists of:

– the CHB-MIT Scalp EEG database [9]: The dataset consists of EEG recordings from 22 pediatric subjects with intractable epilepsy collected by the Boston Children's Hospital and detailed in [8]. The recordings were obtained by monitoring the subjects for up to several days after discontinuation of anti-epileptic drugs to characterize their seizures and assess their suitability for surgical intervention. A total of 22 subjects (5 males, ages 3-22 years; 17 females, ages 1.5-19). In this experiment, five subjects were randomly selected for numerical experimentation and model validation; distribution of the different genders and ages to test the generalization of the model is shown in Table 1. For each data set in the table, we used 80% for training and the remaining 20% for testing.

Table 1. Information on five subjects

Subject	Age	Gender	EEG seconds	Number of seizures	Seizure seconds	Proportion
chb01	11	female	23925	7	442	1.85%
chb02	11	male	8159	3	172	2.11%
chb03	14	female	25200	7	402	1.60%
chb05	7	female	18000	5	558	3.1%
chb08	3.5	male	18000	5	919	5.11%
chb_5_mix	-	-	93284	27	2493	2.67%

– the Helsinki University Hospital (HUH) neonatal epilepsy dataset [33]: this dataset consists of EEG recordings from 79 infants admitted to the NICU at the HUH between 2010 and 2014. These recordings were separately annotated by three experts and hence contains discrepancies between the labeled EEG traces. On average, a total of 460 seizures were annotated per expert; out of this, 39 neonates had seizures and 22 were seizure free, by consensus. This situation with the dataset labels enables us to compare the labels from different experts with our model classification results; for this work, we randomly sampled 10 datapoints, from both male and female neonates, respectively, so as to ensure fullest possible coverage of the dataset.

3.2 Model Training

The model was trained and tested on a single GPU (RTX 4090 24GB) using the Pytorch and braindecode [28] frameworks. For all experiments, we used the following training configuration: the training was done using the Adam optimizer and the cross-entropy loss function with a learning rate of 0.0001, a batch size of 64, and training for 20 epochs. We also tried several different configurations of hyperparameters, the training results from which is detailed in the Results section. In addition, the pre-processing of all EEG data only uses a bandpass filter for 8-30Hz filtering

3.3 Model Overview

TSICNet Here we describe the TSICNet in detail. The primary submodule in TSICNet is a temporal convolutional layer with the kernel size set to $(1, 64)$; it extracts time domain features and outputs N feature maps. Since the convolution kernel size is $(1, 64)$ and the sampling rate is 256, information above 4Hz can be extracted. The extracted features are input into the spatial GCNN. In the GCNN, given the graph $G = (V, E)$, where V represents the set of nodes, and E represents the set of edges between nodes in E, V data can be used on the matrix $X \in \mathbb{R}^{n \times d}$, where $n = |V|$ and d the input feature dimension. The edge set E can be used to construct the the weighted adjacency matrix $A \in \mathbb{R}^{n \times n}$, where $A_{ii} = 1$, $i = 1, 2, \ldots, n$. The data in other positions of the matrix are Pearson correlation coefficients. On the other hand, the GCNN learns elements of the matrix $I \in \mathbb{R}^{n \times n}$, namely the importance matrix. I can be understood as a measure of the importance of different input channels for the connection of different nodes (or edges) in the graph. Between adjacent layers of GNN, the feature transformation can be written as:

$$Z^{l+1} = Z^{l}(A \odot I) \tag{1}$$

where $l = 0, 1, \ldots, l-1, l$ and $Z^0 = X$, $H^L = Z$, I to learn the importance of the matrix. The Pearson correlation coefficient is a number between -1 and 1 that measures the strength of the linear relationship between two variables. When this coefficient is positive, it means that there is a positive correlation between

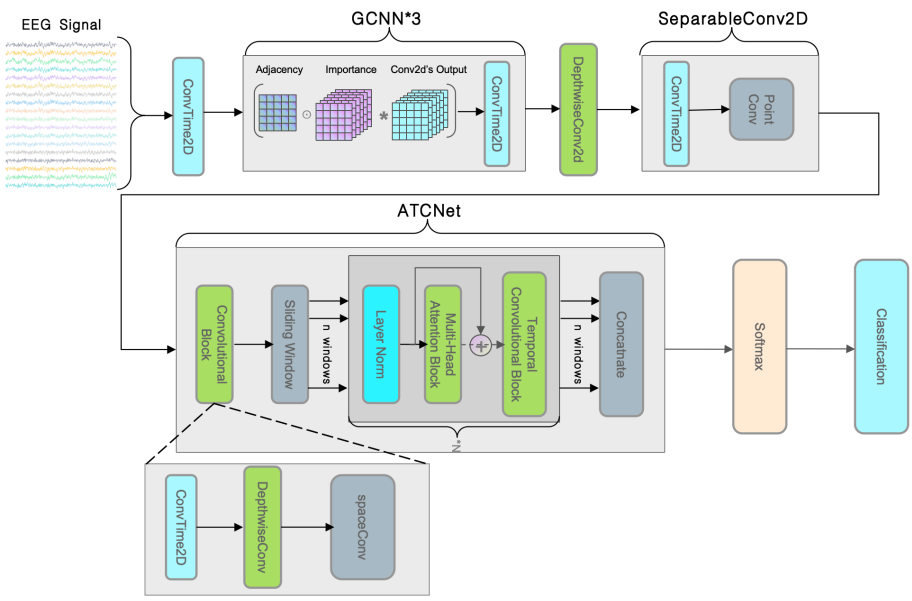

Fig. 1. TSICNet structure diagram

the two variables, and conversely. If the value is 0, there is no linear relationship between the two variables. The mathematical formula for Pearson's correlation coefficient is:

$$r = \frac{\sum_{i=1}^{n}(x_i - \bar{x})(y_i - \bar{y})}{\sqrt{\sum_{i=1}^{n}(x_i - \bar{x})^2}\sqrt{\sum_{i=1}^{n}(y_i - \bar{y})^2}} \tag{2}$$

n is the number of samples, x_i and y_i are the first I observations of the two variables under consideration, and x, y the respective sample means. From this, we establish an correlation adjacency matrix with a size of $[23, 23]$ as shown in Figure 2, where the value 23 represents the number of sensor channels in the CHB-MIT Scalp EEG setup. Each value of r_{ij} in the matrix represents the correlation between the first i and j EEG channels. Since we regard the EEG channels as an undirected graph, the adjacency matrix is symmetric with a unit diagonal. As shown in Eq. 1, I initializes a square coefficient matrix in the network that can be updated as the network learns, with its initial values randomly drawn from the standard normal distribution. The A is a learnable prefactor that adjusts the importance between different nodes so that the adjacency matrix becomes fully adaptive according to the input data. It is elementwise-multiplied by the importance matrix I; this operation weights the adjacency matrix, with the weights provided by I. This means that different input channels will have different effects on the connections in the diagram, and this effect is learned. Finally, the result is multiplied by the EEG dataset matrix after convolution and batch normalization.

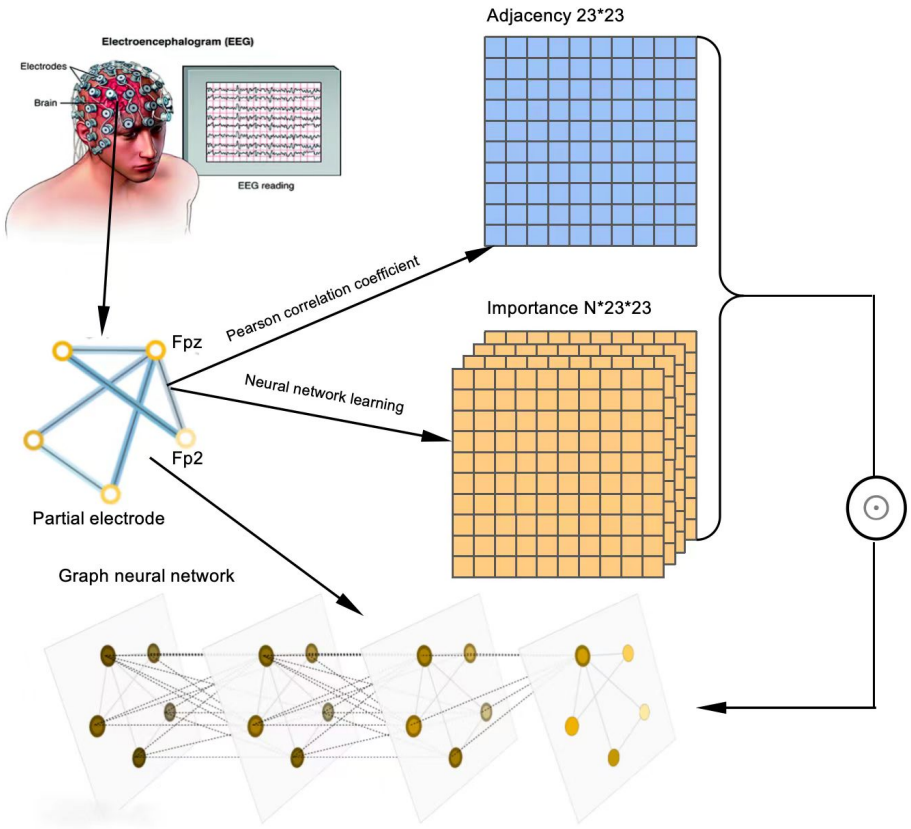

Fig. 2. The relationship between connectomic information from EEG traces and the adjacency matrix in TSICNet.

By making I a learnable parameter, the model adaptively adjusts the structure of the graph during training. This allows the model to learn which input channels are more important for a particular graph connection, thereby better capturing the relationship between the graph structure and the input data. Multiplying the weighted adjacency matrix with the input data $\mathbf{x}$ actually fuses the structure information of the graph with the input data. This fusion allows the model to consider both the structure of the graph and the characteristics of the input data, allowing for more complex classification tasks.

The final layer in TSICNet is a separable convolution that explicitly decouples relationships within and between feature maps by first learning a kernel that individually summarizes each feature map and then merges the results to produce an output.

4 Results

4.1 Baseline Models

We perform extensive experiments comparing the performance of TSICNet with a number of SOTA baseline models. All of these baselines are models that were optimized for tasks on EEG data. Apart from this set of conventional deep EEG models, we also compared TSICNet with a group of GCNN-based deep models. These models are briefly described in the following:

- ATCNet [2]: ATCNet is an attention-based framework for motor imagery classification. The framework consists of self-attention, temporal convolution submodules for feature extraction, and includes a convolutional-layer-based sliding window for data augmentation;
- EEGNet [15]: the EEGNet is a classic deep model for EEG tasks. The backbone of this model are convolutional layers which are organized serially in such a way to enhance generalizability across different BCI paradigms;
- EEGInception [26]: the EEG-Inception model fuses conventional convolutional layers in a chain of Inception modules, and optimized for event-related potential (ERP) tasks. The Inception modules are chosen for their multiscale feature resolution;
- EEG-ITNet [25]: this model is also based on the Inception framework, augmented by causal convolutions with dilations. The authors of this paper have also developed a visualization method for more effective EEG analysis result interpretation;
- EEGConformer [31]: the EEGConformer is a novel architecture based on convolutional transformer submodules, in which the convolutional layers learn the low-level local features, while the self-attention modules extracts the global correlations within the local features;

Apart from the deep EEG models listed above, we also compared TSICNet to several GCNN-based models.

- AST-GCN [38]: the AST-GCN is a graph-convolutional network for traffic forecasting. It consists of static and dynamic attribute augmentation module which integrates external factors for input to a conventional spatio-temporal GCN;
- AS-GCN [37]: the AS-GCN is a text dependency-tree based model which learns syntactical and word-level relations in sentences, which is then applied to a sentiment-classification task;
- ST-GCN [10]: the ST-GCN can be considered to be the original graph-convolutional based model which takes both spatial and temporal relationships between nodes into account. The original task, as reported in this publication, was for point-of-interest (POI) recommendation.

4.2 Comparison with Baseline Models

We compare the TSICNet with several baseline models on the CHB-MIT dataset. In addition to the accuracy, we also compute the True $TPR = \frac{TP}{TP+FN}$ and False Positive Rates $FPR = \frac{FP}{FP+TN}$ indicators. These are are commonly used in binary classification tasks to complement ROC curves. Here TP (True Positive) indicates the number of samples that are positive and returned by the model, and FN (False Negative) indicates the number of samples that are actually positive but computed by the model to be negative. The other two classes, FP (False Positive) and TN (True Negative) can be obtained by taking the complement of the normalized values of these factors. Table 2 shows a comparison of our model to several baseline, SOTA models, evaluated on the CHB-MIT dataset. Results obtained in this table are averaged values over the full sampled patient cohort. We see that our model achieves superior accuracy compared to the baselines; this is true as well in terms of the TPR and FPR factors. We consider the evaluation of TPR and FPR in order to mitigate the problem of our model overfitting on the majority label, given that the labels in our dataset is significantly unbalanced. In Table 4 we report on results on individual members of the sampled cohort; the column labeled `chb_5_mix` is a special instance constructed by mixing sampled data from the individual members of the cohort; results of model evaluation on this constructed cohort is meant to be indicative of the generalizability of our model. From Table 4 it is clear that the performance of our model is transferable across patients, indicating a high level of model generalizability on this cohort. Figure 3 show the six confusion matrices corresponding to the models under evaluation. We see that, in terms of absolute numbers, the FPs and TNs obtained from our model are an order of magnitude smaller than other baseline models, indicating the robustness of TSICNet under real use cases. Table 3 shows model

Table 2. Performance comparison of baseline models with TSICNet on the CHB-MIT dataset

-	TSICNet	ATCNet	EEGNet	EEGInception	EEGITNet	EEGConformer
Accuracy	**99.90%**	98.10%	98.08%	97.85%	97.32%	98.51%
TPR	**99.72%**	56.25%	70.31%	70.17%	32.10%	78.55%
FPR	0.09%	0.22%	0.81%	1.04%	**0.07%**	0.69%

evaluation and baseline comparison on the HUH dataset. For this dataset, we randomly sampled ten individuals (ten male and ten female), in order to show that our model generalizability systematically transfers across gender as well as samples. We see that again, for this dataset we are able to achieve full SOTA accuracies and TPR/FPR numbers (performance of our model is shown in the first column).

Table 3. Performance comparison of baseline models with TSICNet on the HUH dataset

	Subject	TSICNet			ATCNet			EEGNet			EEGInception			EEGITNet			EEGConformer		
		ACC	TPR	FPR	ACC	TPR	FPR	ACC	TPR	FPR	ACC	TPR	FPR	ACC	TPR	FPR	ACC	TPR	FPR
Female	1	99.60%	99.07%	0.08%	98.20%	97.88%	1.60%	95.10%	92.43%	3.29%	89.80%	72.90%	0.06%	91.40%	87.12%	6.01%	99.10%	98.80%	0.72%
	5	99.95%	99.92%	0.06%	99.95%	99.95%	0.00%	99.90%	99.89%	0.00%	99.95%	99.92%	0.06%	79.80%	78.44%	0.00%	99.95%	99.92%	0.00%
	9	99.95%	99.42%	0.00%	99.95%	99.42%	0.00%	99.80%	98.28%	0.05%	96.45%	59.20%	0.00%	97.65%	72.99%	0.00%	99.85%	98.85%	0.05%
	14	99.50%	99.09%	0.10%	99.50%	99.29%	0.30%	99.00%	98.68%	0.69%	98.80%	97.87%	0.30%	88.25%	76.21%	0.00%	99.60%	99.60%	0.40%
	17	99.70%	90.62%	0.00%	99.85%	99.90%	0.15%	99.80%	98.43%	0.21%	99.65%	89.06%	0.00%	97.35%	17.19%	0.00%	99.65%	95.31%	0.21%
	19	99.90%	95.83%	0.00%	99.95%	99.92%	0.00%	99.95%	99.92%	0.05%	99.80%	91.67%	0.00%	99.80%	91.67%	0.00%	99.95%	99.92%	0.00%
	22	99.65%	99.81%	0.41%	99.40%	99.92%	0.82%	99.60%	99.81%	0.48%	98.90%	96.10%	0.07%	90.90%	99.63%	12.31%	99.65%	99.92%	0.48%
	31	99.95%	99.92%	0.00%	99.95%	99.92%	0.00%	99.80%	98.35%	0.06%	99.00%	89.01%	0.00%	97.30%	70.33%	0.00%	99.95%	99.45%	0.00%
	41	99.80%	99.78%	0.00%	99.25%	99.78%	5.37%	99.15%	99.39%	2.99%	95.50%	99.96%	44.78%	77.55%	75.04%	0.00%	99.80%	99.89%	1.00%
	44	99.20%	86.55%	0.00%	97.55%	58.82%	0.00%	94.40%	5.88%	0.00%	85.80%	99.65%	15.10%	94.05%	0.00%	0.00%	99.75%	99.90%	0.27%
	F_Avg	**99.72**%	97.00%	**0.06**%	99.36%	95.49%	0.82%	98.65%	89.13%	0.78%	96.37%	89.58%	6.03%	91.41%	66.86%	1.83%	**99.72**%	**99.17**%	0.31%
Male	4	99.95%	99.92%	0.07%	99.95%	99.92%	0.00%	99.90%	99.92%	0.14%	98.55%	94.56%	0.00%	92.20%	70.73%	0.00%	99.95%	99.61%	0.00%
	7	99.95%	99.78%	0.00%	99.85%	99.78%	0.13%	99.80%	99.56%	0.13%	98.60%	93.89%	0.00%	99.60%	98.25%	0.00%	99.90%	99.78%	0.06%
	15	99.75%	99.20%	0.12%	99.70%	99.47%	0.25%	99.35%	97.86%	0.31%	88.65%	100%	13.96%	95.35%	75.13%	0.00%	99.65%	98.40%	0.06%
	16	99.15%	94.76%	0.17%	98.15%	98.88%	1.96%	98.10%	92.13%	0.98%	98.80%	97.75%	1.04%	89.60%	22.10%	0.00%	98.90%	96.63%	0.75%
	20	99.35%	96.67%	0.18%	99.45%	98.67%	0.41%	98.40%	91.00%	0.29%	99.25%	95.33%	0.06%	97.00%	80.67%	0.12%	99.90%	98.00%	0.24%
	21	99.95%	99.92%	0.00%	99.95%	99.92%	0.00%	99.95%	99.92%	0.00%	99.95%	99.92%	0.05%	99.85%	93.02%	0.00%	99.95%	99.92%	0.00%
	38	99.85%	99.87%	0.21%	99.75%	99.92%	0.31%	99.35%	96.58%	0.00%	94.45%	70.79%	0.00%	85.20%	22.11%	0.00%	99.30%	96.84%	0.12%
	39	99.40%	96.75%	0.06%	99.15%	95.56%	0.12%	96.4%	78.70%	0.00%	99.10%	94.67%	0.00%	86.20%	18.34%	0.00%	98.75%	94.38%	0.36%
	40	99.85%	99.35%	0.00%	99.10%	96.56%	0.13%	93.35%	71.83%	0.13%	86.20%	40.65%	0.00%	97.80%	91.61%	0.46%	99.45%	99.57%	0.59%
	52	99.90%	98.32%	0.00%	99.95%	99.92%	0.00%	99.95%	100%	0.05%	99.40%	89.92%	0.00%	99.15%	85.71%	0.00%	99.95%	99.92%	0.00%
	M_Avg	**99.71**%	98.46%	0.08%	99.50%	**98.87**%	0.33%	98.46%	92.77%	0.20%	93.30%	87.76%	1.51%	94.20%	71.80%	**0.06**%	99.57%	98.30%	0.22%
	Avg	**99.72**%	97.73%	**0.07**%	99.43%	97.18%	0.58%	98.56%	90.95%	0.49%	94.84%	88.67%	3.77%	92.80%	69.33%	0.95%	99.66%	**98.74**%	0.27%

Fig. 3. The confusion matrix of 6 different models, from left to right and from top to bottom, is TSICNet, ATCNet, EEGNet, EEGInception, EEGITNet, and EEGConformer.

4.3 Comparison with Graph-Convolution-Based Models

In addition to conventional deep models for EEG analysis, we also compared our model design with three existing combination GCNN models; this was done in order to verify the validity of our design principles (as mentioned in the model

Table 4. Data set results for a single subject and a mix of five subjects

-	chb_5_mix	chb01	chb02	chb03	chb05	chb08
Accuracy	99.90%	99.48%	99.63%	99.69%	99.72%	99.98%
TPR	99.72%	98.02%	97.55%	95.70%	96.37%	99.96%
FPR	0.09%	0.45%	0.30%	0.24%	0.17%	0.05%

description section), in particular with respect to the inclusion and training of the GCNN. The results are reported in Table 5 and confirms the superiority of our proposed combined GCNN architecture. We note that some of the GCNN-based models examined under this study have structures similar to ours; e.g., the ASTGCNN [38] is also a fusion of graph convolution with the attention mechanism, while the STGCNN [10] learns relationships between both spatial and temporal points, similarly to the way we integrate this information via spatial and temporal convolutional layers in the TSICNet.

Table 5. Performance comparison of four models combined with GCNN

-	TSICNet	ASTGCNN	ASGCNN	STGCNN
Accuracy	**99.55%**	97.89%	96.77%	98.90%
TPR	**96.73%**	72.34%	68.55%	75.99%
FPR	0.34%	0.41%	0.65%	**0.18%**

4.4 Ablation Studies

We performed ablation studies to highlight the roles of the different modules in achieving our reported classification results. Overall ablation results, reported in Table 6, show the decrease in accuracy and TPR / FPR when we remove different submodules from our framework; this indicates the efficacy of our model design principles in translation to actual results. We note that a larger decrease in performance was observed when the GCNN was removed as compared to the case when the ATCNet submodule was excised; this indicates the importance of the connectome learning module (implemented in the adjacency matrix of the GCNN) in our model's results, and validates the hypothesis forming the major basis of our model design. Removal of additional submodules led to larger decrease in accuracy, which is to be expected.

Decoding Methods Data extraction for model training was conducted using various sliding windows in the CHB-MIT Scalp dataset, with each window representing a time unit of 1 second. Each time unit comes with its own label (seizure or no seizure). We ablate with respect to three types of sliding Windows: in the

Table 6. TSICNet Ablation Studies

Removed	Accuracy	TPR	FPR
None	99.90%	99.72%	0.18%
ATCNet	99.55%	96.73%	0.34%
GCNN	99.06%	83.52%	0.31%
ATCNet+GCNN	98.08%	70.31%	0.81%
Conv+GCNN	98.10%	56.25%	0.22%

first case, each window includes 1 second of data, the step length is 1 (full length of the window), and the label of this second is fixed by this data. In the second method, each window contains 6 seconds of data and the step size is 1 second, while in the final case we add 4 seconds of data on the basis of the second window, and the step length is 1 second, that is, a total of 10 seconds of data to judge the 5 to 6 seconds of labels in the window. The schematic diagram of the three sliding windows is shown in Figure 4

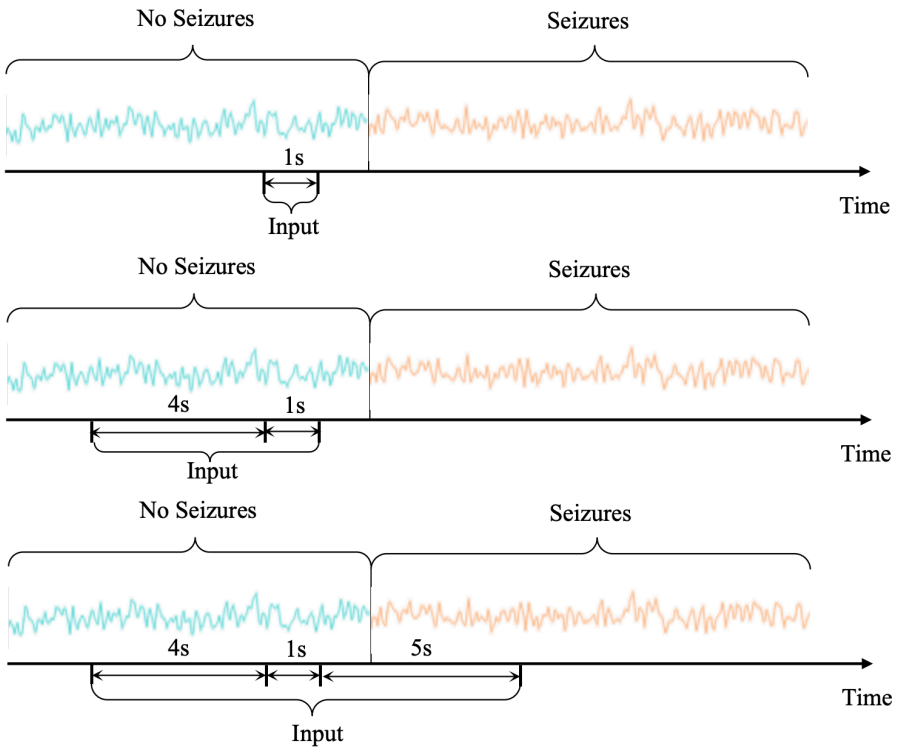

Fig. 4. Schematic comparison between our three sliding windows information extraction schemes.

From this set of ablation results we observe an expected increase in model accuracy with amount of training data, although the variance between these sets are not substantial. However, we do observe a sharp drop in the TPR when reducing the length of the learning window, which is indicative of increasing overfitting. The experimental results are shown in Table 7.

Table 7. Performance comparison of different sliding windows

-	10sec	6sec	1sec
Accuracy	**99.75%**	99.35%	99.17%
TPR	**99.71%**	96.16%	90.63%
FPR	**0.20%**	0.52%	0.48%

Feature extraction and learning from ATCNet and TSICNet As our TSICNet design incorporates parts ofthe existing ATCNet, the question of how to integrate both these modules is of interest. We studied four different combination methodologies, the first two being combination in series, but in various different orders; the latter two involves combinations in parallel and applying either addition or concatenation to the resulting learned feature vectors for feature fusion. The experimental comparison results of the four combination methods are shown in Table 8. It can be seen that a series combination method with ATCNet at the end is the best combination method.

Table 8. Comparison of different combinations of ATCNet

-	ATCNet (back)	ATCNet (front)	Concatenation	Addition
Accuracy	**99.90%**	99.06%	99.64%	99.75%
TPR	**99.72%**	78.55%	96.78%	99.71%
FPR	**0.09%**	0.36%	0.24%	0.20%

5 Conclusion

Epilepsy is one of the most prevalent neurological diseases, affecting millions of people worldwide and imposing substantial social and economic burdens. In recent years, deep learning methods have become widely applied in numerous areas of scientific research, due, in part, to its ability to automatically extract the most relevant features and the availability of extensive, multimodal datasets for almost all areas. In this work, we have endeavoured to take advantage of this feature learning capability of deep learning and incorporate, as far as possible,

important prior knowledge and information regarding epilepsy. Based on these considerations, we design TSICNet, a novel framework for epilepsy classification which is able to: first, capture the main indicators of an epileptic seizures, and second, extract the most relevant features according to these indicators. The main design principles involved combines key features from various elemental modules to maximize the accuracy of model classification; for this task, our model combines CSP capabilities with connectomic and multi-level attention in order to maximize the amount of relevant extracted information. Comparison with baseline models show SOTA performance in comparison with five current models, each based on various different learning structures. Comparison with GCNN-based deep models also substantiate our reasoning regarding the use of graph-based layers in our model. Finally, ablation studies show the efficacy of our design principles from various perspectives. We regard this work as a hint towards the possibility of robust and accurate epilepsy diagnosis models, by basing model design principles on knowledge and understanding of prior medical information and data.

Disclosure of Interests. There are no conflicts of interests

References

1. Acharya, U.R., Hagiwara, Y., Adeli, H.: Automated seizure prediction. Epilepsy Behav **88**, 251–261 (2018). https://doi.org/10.1016/j.yebeh.2018.09.030
2. Altaheri, H., Muhammad, G., Alsulaiman, M.: Physics-informed attention temporal convolutional network for eeg-based motor imagery classification. IEEE transactions on industrial informatics **19**(2), 2249–2258 (2022)
3. Bhattacharya, A., Baweja, T., Karri, S.P.K.: Epileptic seizure prediction using deep transformer model. International Journal of Neural Systems **32**(02), 2150058 (2022). https://doi.org/10.1142/S0129065721500581, https://doi.org/10.1142/S0129065721500581, pMID: 34720065
4. Blume, W.T.: Diagnosis and management of epilepsy. CMAJ **168**(4), 441–448 (Feb 2003)
5. Bonilha, L., Jensen, J.H., Baker, N., Breedlove, J., Nesland, T., Lin, J.J., Drane, D.L., Saindane, A.M., Binder, J.R., Kuzniecky, R.I.: The brain connectome as a personalized biomarker of seizure outcomes after temporal lobectomy. Neurology **84**(18), 1846–1853 (2015). https://doi.org/10.1212/WNL.0000000000001548, https://www.neurology.org/doi/abs/10.1212/WNL.0000000000001548
6. D.K., T., B.G., P., Xiong, F.: Epileptic seizure detection and prediction using stacked bidirectional long short term memory. Pattern Recognition Letters **128**, 529–535 (2019). https://doi.org/https://doi.org/10.1016/j.patrec.2019.10.034, https://www.sciencedirect.com/science/article/pii/S0167865519303125
7. Fisher, R.S., et al.: Ilae official report: a practical clinical definition of epilepsy. Epilepsia **55**(4), 475–482 (2014). https://doi.org/10.1111/epi.12550
8. Goldberger, A.L., Amaral, L., Glass, L., Hausdorff, J., Ivanov, P.C., Mark, R., ..., Stanley, H.E.: PhysioBank, PhysioToolkit, and PhysioNet: Components of a new research resource for complex physiologic signals. Circulation [Online] **101**(23), e215–e220 (2000)

9. Guttag, J.: CHB-MIT Scalp EEG Database (version 1.0.0). PhysioNet (2010), https://doi.org/10.13026/C2K01R
10. Han, H., Zhang, M., Hou, M., Zhang, F., Wang, Z., Chen, E., Wang, H., Ma, J., Liu, Q.: Stgcn: a spatial-temporal aware graph learning method for poi recommendation. In: 2020 IEEE International Conference on Data Mining (ICDM). pp. 1052–1057. IEEE (2020)
11. Hussein, R., Palangi, H., Ward, R.K., Wang, Z.J.: Optimized deep neural network architecture for robust detection of epileptic seizures using eeg signals. Clinical Neurophysiology **130**(1), 25–37 (2019). https://doi.org/https://doi.org/10.1016/j.clinph.2018.10.010, https://www.sciencedirect.com/science/article/pii/S1388245718313464
12. Iasemidis, L., Sabesan, S., Good, L., Chakravarthy, N., Treiman, D., Sirven, J., Tsakalis, K.: Seizures | a new look into epilepsy as a dynamical disorder : Seizure prediction, resetting and control. In: Schwartzkroin, P.A. (ed.) Encyclopedia of Basic Epilepsy Research, pp. 1295–1302. Academic Press, Oxford (2009). https://doi.org/https://doi.org/10.1016/B978-012373961-2.00267-8, https://www.sciencedirect.com/science/article/pii/B9780123739612002678
13. Johansen, A.R., Jin, J., Maszczyk, T., Dauwels, J., Cash, S., Westover, M.: Epileptiform spike detection via convolutional neural networks. In: Proc IEEE Int Conf Acoust Speech Signal Process. vol. 2016, pp. 754–758 (2016). https://doi.org/10.1109/ICASSP.2016.7471776
14. Kiral-Kornek, I., Roy, S., Nurse, E., Mashford, B., Karoly, P., Carroll, T., Payne, D., Saha, S., Baldassano, S., O'Brien, T., Grayden, D., Cook, M., Freestone, D., Harrer, S.: Epileptic seizure prediction using big data and deep learning: Toward a mobile system. EBioMedicine **27**, 103–111 (2018). https://doi.org/https://doi.org/10.1016/j.ebiom.2017.11.032, https://www.sciencedirect.com/science/article/pii/S235239641730470X
15. Lawhern, V.J., Solon, A.J., Waytowich, N.R., Gordon, S.M., Hung, C.P., Lance, B.J.: Eegnet: a compact convolutional neural network for eeg-based brain–computer interfaces. Journal of neural engineering **15**(5), 056013 (2018)
16. Li, X., Xiong, H., Li, X., Wu, X., Zhang, X., Liu, J., Bian, J., Dou, D.: Interpretable deep learning: interpretation, interpretability, trustworthiness, and beyond. Knowledge and Information Systems **64**(12), 3197–3234 (2022). https://doi.org/10.1007/s10115-022-01756-8, https://doi.org/10.1007/s10115-022-01756-8
17. Maher, C., Tang, Z., DSouza, A., Cabezas, M., Cai, W., Barnett, M., Kavehei, O., Wang, C., Nikpour, A.: Deep learning distinguishes connectomes from focal epilepsy patients and controls: feasibility and clinical implications. Brain Communications **5**(6), fcad294 (10 2023). https://doi.org/10.1093/braincomms/fcad294, https://doi.org/10.1093/braincomms/fcad294
18. Mallick, S., Baths, V.: Novel deep learning framework for detection of epileptic seizures using eeg signals. Frontiers in Computational Neuroscience **18** (2024). https://doi.org/10.3389/fncom.2024.1340251, https://www.frontiersin.org/articles/10.3389/fncom.2024.1340251
19. Manole, A.M., Sirbu, C.A., Mititelu, M.R., Vasiliu, O., Lorusso, L., Sirbu, O.M., Ionita Radu, F.: State of the art and challenges in epilepsya narrative review. J. Pers. Med. **13**(4), 623 (2023). https://doi.org/10.3390/jpm13040623, https://doi.org/10.3390/jpm13040623
20. Morgan, V.L., et al.: Presurgical temporal lobe epilepsy connectome fingerprint for seizure outcome prediction. Brain communications **4**(3), fcac128 (2022). https://doi.org/10.1093/braincomms/fcac128

21. Orhan, U., Hekim, M., Ozer, M.: Eeg signals classification using the k-means clustering and a multilayer perceptron neural network model. Expert Systems with Applications **38**(10), 13475–13481 (2011). https://doi.org/https://doi.org/10.1016/j.eswa.2011.04.149, https://www.sciencedirect.com/science/article/pii/S0957417411006762
22. Ouichka, O., Echtioui, A., Hamam, H.: Deep learning models for predicting epileptic seizures using ieeg signals. Electronics **11**(4), 605 (2022). https://doi.org/10.3390/electronics11040605, https://doi.org/10.3390/electronics11040605
23. Proix, T., Jirsa, V.K.: Using the connectome to predict epileptic seizure propagation in the human brain. BMC Neurosci **16**(Suppl 1), P110 (2015). https://doi.org/10.1186/1471-2202-16-S1-P110, https://doi.org/10.1186/1471-2202-16-S1-P110
24. Roy, S., Kiral-Kornek, I., Harrer, S.: Chrononet: A deep recurrent neural network for abnormal eeg identification. In: Riaño, D., Wilk, S., ten Teije, A. (eds.) Artificial Intelligence in Medicine. AIME 2019. vol. 11526. Springer, Cham (2019). https://doi.org/10.1007/978-3-030-21642-9_8, https://doi.org/10.1007/978-3-030-21642-9-8
25. Salami, A., Andreu-Perez, J., Gillmeister, H.: Eeg-itnet: An explainable inception temporal convolutional network for motor imagery classification. IEEE Access **10**, 36672–36685 (2022)
26. Santamaria-Vazquez, E., Martinez-Cagigal, V., Vaquerizo-Villar, F., Hornero, R.: Eeg-inception: a novel deep convolutional neural network for assistive erp-based brain-computer interfaces. IEEE Transactions on Neural Systems and Rehabilitation Engineering **28**(12), 2773–2782 (2020)
27. Scharfman, H.E.: The neurobiology of epilepsy. Curr Neurol Neurosci Rep **7**(4), 348–354 (2007). https://doi.org/10.1007/s11910-007-0053-z
28. Schirrmeister, R.T., Springenberg, J.T., Fiederer, L.D.J., Glasstetter, M., Eggensperger, K., Tangermann, M., Hutter, F., Burgard, W., Ball, T.: Deep learning with convolutional neural networks for eeg decoding and visualization. Human Brain Mapping (aug 2017). https://doi.org/10.1002/hbm.23730, http://dx.doi.org/10.1002/hbm.23730
29. Shoeibi, A., Moridian, P., Khodatars, M., Ghassemi, N., Jafari, M., Alizadehsani, R., Kong, Y., Gorriz, J.M., Ramírez, J., Khosravi, A., Nahavandi, S., Acharya, U.R.: An overview of deep learning techniques for epileptic seizures detection and prediction based on neuroimaging modalities: Methods, challenges, and future works. Comput. Biol. Med. **149**(C) (oct 2022). https://doi.org/10.1016/j.compbiomed.2022.106053, https://doi.org/10.1016/j.compbiomed.2022.106053
30. Singh, A., Velagala, V.R., Kumar, T., et al.: The application of deep learning to electroencephalograms, magnetic resonance imaging, and implants for the detection of epileptic seizures: A narrative review. Cureus **15**(7), e42460 (2023). https://doi.org/10.7759/cureus.42460
31. Song, Y., Zheng, Q., Liu, B., Gao, X.: Eeg conformer: Convolutional transformer for eeg decoding and visualization. IEEE Transactions on Neural Systems and Rehabilitation Engineering **31**, 710–719 (2022)
32. Stafstrom, C.E., Carmant, L.: Seizures and epilepsy: An overview for neuroscientists. Cold Spring Harb Perspect Med **5**(6), a022426 (2015). https://doi.org/10.1101/cshperspect.a022426

33. Stevenson, N.J., Tapani, K., Lauronen, L., Vanhatalo, S.: A dataset of neonatal eeg recordings with seizure annotations. Sci Data **6**, 190039 (2019). https://doi.org/10.1038/sdata.2019.39
34. Tzallas, A.T., Tsipouras, M.G., Fotiadis, D.I.: Automatic seizure detection based on time-frequency analysis and artificial neural networks. Comput Intell Neurosci **2007**, 80510 (2007). https://doi.org/10.1155/2007/80510
35. Ullah, I., Hussain, M., ul Haq Qazi, E., Aboalsamh, H.: An automated system for epilepsy detection using eeg brain signals based on deep learning approach. Expert Systems with Applications **107**, 61–71 (2018). https://doi.org/https://doi.org/10.1016/j.eswa.2018.04.021, https://www.sciencedirect.com/science/article/pii/S0957417418302513
36. West, J., Bozorgi, Z.D., Herron, J., Chizeck, H.J., Chambers, J.D., Li, L.: Machine learning seizure prediction: one problematic but accepted practice. Journal of Neural Engineering **20**(1), 016008 (jan 2023). https://doi.org/10.1088/1741-2552/acae09, https://dx.doi.org/10.1088/1741-2552/acae09
37. Zhang, C., Li, Q., Song, D.: Aspect-based sentiment classification with aspect-specific graph convolutional networks. arXiv preprint arXiv:1909.03477 (2019)
38. Zhu, J., Wang, Q., Tao, C., Deng, H., Zhao, L., Li, H.: Ast-gcn: Attribute-augmented spatiotemporal graph convolutional network for traffic forecasting. Ieee Access **9**, 35973–35983 (2021)